MJFAS
Malaysian Journal of Fundamental and Applied Sciences

Kunasegaran *et al.* | Malaysian Journal of Fundamental and Applied Sciences, Vol. 22 (2026) 298–308

RESEARCH ARTICLE

Analytical Solution of Two-Dimensional Advection-Diffusion Equation with Caputo-Fabrizio Derivative and Time Dependent Velocity

Purani Kunasegaran[a], Zaiton Mat Isa[a,b,*]

[a]Department of Mathematical Sciences, Faculty of Science, Universiti Teknologi Malaysia, 81310 UTM Johor Bahru, Johor, Malaysia; [b]UTM Center for Industrial and Applied Mathematics (UTM-CIAM), Ibnu Sina Institute for Scientific and Industrial Research, Universiti Teknologi Malaysia, 81310 UTM Johor Bahru, Johor, Malaysia

Abstract The advection-diffusion equation (ADE) is a fundamental mathematical model that is widely used to describe the transport of substances, such as the transport of pollutants in rivers, groundwater or soil. Incorporating a fractional derivative into the ADE allows for non-integer orders which have been demonstrated to capture more complex dynamics that cannot be described by classical ADE. This study investigates a two-dimensional ADE with time-fractional Caputo-Fabrizio derivative while considering a time-dependent velocity. The velocity function varies temporally, while the diffusion coefficient remains constant. By introducing appropriate transformations, the equation is reformulated and reduced to an equation with constant coefficients. Analytical solutions are obtained using the Laplace transform in time and the Fourier transform in spatial coordinates. The derived solutions encompass classical and fractional advection-diffusion processes, highlighting the impact of fractional-order derivatives. Numerical simulations illustrate the influence of time-dependent velocity on concentration profiles, providing a comparative analysis. The results show that lower fractional parameter values yield lower concentration profiles in both spatial domains, with a peak around the centerline and the source. As time increases, the fractional solutions maintain a localized concentration near the centerline and the source, while the classical solution becomes more flattened and moves further downstream. Additionally, a time-dependent velocity consistently yields higher concentration profiles than a constant velocity. These results offer valuable insights into the role of fractional calculus in modeling transport processes with evolving velocity fields, contributing to both theoretical advancements and practical applications in environmental and engineering sciences.

Keywords: Advection-Diffusion Equation, Caputo-Fabrizio Fractional Derivative, Time Dependent, Laplace Transform, Fourier Transform.

***For correspondence:**
zaitonmi@utm.my

Received: 20 June 2025
Accepted: 13 March 2026

Introduction

The advection-diffusion equation (ADE) describes the transport process due to the combined influences of advection and diffusion. Diffusion is the process by which matter is transported from high concentration to low concentration through random molecular motions. Meanwhile, advection is the process where a substance is transported by the movement of a fluid or solvent. Its analytical and numerical solutions have drawn the attention of many authors, since the ADE has a broad range of applications. For example, ADE has assisted in understanding the concentration of pollutant in the river ([1]; [2]; [3]; [4]) and in soil ([5]; [6]). Besides, mathematical modelling based on ADE also has been implemented in investigating the concentration of contaminant in groundwater ([7]; [8]; [9];[10];[11]).

In recent years, there has been growing interest in studying fractional ADE (FADE). FADE that offers non-integer orders, has advantages that can capture non-local behaviour, which may not be captured by the classical ADE. Studies also have shown that fractional derivatives lead to a better fit of the experimental data than the classical ADE. In the study by [12], it was found that compared to advection - dispersion equation model, fractional advection-dispersion equation model provides better simulation for the concentration in breakthrough curves for adsorbing contaminant. Also, while investigating the transport of solute in a fracture using the FADE, [30] compared the results with the classical ADE. The findings show that FADE provides a better fit than the ADE based on their validation with experimental data. Meanwhile [13] in his book shows how fractional calculus offers a suitable (albeit frequently empirical) method for describing the dynamic characteristics of linear viscoelastic media including problems of wave propagation and diffusion.

Thus far, several studies have explored the solutions and properties of FADE using various analytical and numerical techniques. Analytically, [14] and [15] derived the solution for a two-dimensional FADE, however it should be noted that their work assumed constant diffusion and advection. Same as in [16], the analytical solutions of Atangana-Baleanu time-fractional derivative ADE is solved for equation where the coefficients are constant. Meanwhile in [17], although a two-dimensional problem is considered, the authors solved the diffusion equation only. The study by [18] formulated the time-fractional ADE using the Caputo fractional derivative and derived the analytical solutions. However, their study solely focused on the one-dimensional domain only. Same as in [19], the presented Caputo left generalized fractional derivative to describe the FADE were solved for problem in one-dimensional space.

It is important to note that diffusion and flow velocity have been proven to vary over time. As a result, some authors have considered variable coefficient with temporally dependent in their study such as in [20], [21], [22], [23], [24] and [25]. However, they obtained solutions to the classical ADE, rather than the fractional derivative in those papers.

In summary, existing analytical solutions to the FADE are primarily limited to one-dimensional problems. In the case of two-dimensional scenarios, coefficients are often assumed to be constant, or the focus is solely on solving the diffusion equation. These limitations highlight the necessity for a more comprehensive analysis that incorporates a two-dimensional framework with time dependent coefficients, providing a more realistic representation of the underlying physical processes.

Based on the above, this proposed study aims to fill these drawbacks by formulating a model equation for a two-dimensional ADE with time dependent velocity incorporating fractional Caputo-Fabrizio derivative. In addition, an instantaneous boundary condition is also introduced to enhance the model's representation. The analytical solutions will be obtained by implementing the Laplace transform and Fourier transform method, motivated upon successful applications in earlier studies ([12]; [14]; [15]; [16]; [26]; [27]).

Definition of Fractional Derivative

The Caputo-Fabrizio (CF) time fractional derivative of order $\alpha \in [0,1)$ is defined as

$$ {}^{CF}D_t^{\alpha} f(t) = \frac{1}{1-\alpha}\int_0^t \exp\left(\frac{-\alpha(t-\tau)}{1-\alpha}\right) f'(\tau)d\tau \tag{1}$$

The Laplace transform of Caputo-Fabrizio time derivative (1) is

$$ L\{ {}^{CF}D_t^{\alpha} f(t)\} = \frac{sL[f(t)] - f(0)}{(1-\alpha)s+\alpha} \tag{2}$$

Remark 1: Taking the limit for $\alpha \to 1$,

$$ \lim_{\alpha\to 1} L\{ {}^{CF}D_t^{\alpha} f(t)\} = sLf(t) - f(0) = L\{f'(t)\} \tag{3}$$

gives the classical ADE.

Mathematical Formulation

A two-dimensional advection-diffusion equation is given by

$$\frac{\partial C(x,y,t)}{\partial t} = D\left[\frac{\partial^2 C(x,y,t)}{\partial x^2} + \frac{\partial^2 C(x,y,t)}{\partial y^2}\right] - u(t)\left[\frac{\partial C(x,y,t)}{\partial x} + \frac{\partial C(x,y,t)}{\partial y}\right] \tag{4}$$

where the $C(x,y,t)$ represents the concentration of the transported substance, u is the velocity field that depends on time, and D is the diffusion coefficient. Initially, there is no concentration in the medium. Also, it is assumed that the concentration source is instantaneously introduced at the boundary. The initial and boundary conditions are considered as

$$C(x,y,0) = 0 \tag{5}$$

$$C(x,0,t) = C_0\delta(x)\delta(t) \tag{6}$$

$$\lim_{x\to\pm\infty} C(x,y,t) = 0, \qquad \lim_{y\to\infty} C(x,y,t) = 0 \tag{7}$$

In the present study, it is assumed that the solute diffusion coefficient remains constant, but the velocity of the flow is temporally dependent, hence

$$D(x,y,t) = D_0 \tag{8}$$

$$u(x,y,t) = u_0 f(mt) \tag{9}$$

Therefore, the (4) assumes the form

$$\frac{\partial C}{\partial t} = D_0\left[\frac{\partial^2 C}{\partial x^2} + \frac{\partial^2 C}{\partial y^2}\right] - u_0 f(mt)\left[\frac{\partial C}{\partial x} + \frac{\partial C}{\partial y}\right] \tag{10}$$

To find the analytical solution, new space variable for X and Y are introduced such that

$$X = \int f(mt)\ dx \tag{11}$$

$$Y = \int f(mt)\, dy \tag{12}$$

The ADE (10) reduces to

$$\frac{1}{f^2(mt)}\frac{\partial C}{\partial t} = D_0\left[\frac{\partial^2 C}{\partial X^2} + \frac{\partial^2 C}{\partial Y^2}\right] - u_0\left[\frac{\partial C}{\partial X} + \frac{\partial C}{\partial Y}\right] \tag{13}$$

Furthermore, a new variable T is introduced by the transformation

$$T = \int_0^t f^2(mt)\, dt \tag{14}$$

which will further reduce (13) as

$$\frac{\partial C}{\partial T} = D_0\left[\frac{\partial^2 C}{\partial X^2} + \frac{\partial^2 C}{\partial Y^2}\right] - u_0\left[\frac{\partial C}{\partial X} + \frac{\partial C}{\partial Y}\right] \tag{15}$$

Meanwhile, the initial and boundary conditions (5) – (7) become

$$C(X,Y,0) = 0 \tag{16}$$

$$C(X,0,T) = \frac{C_0}{a}\delta(X)\delta(T) \tag{17}$$

$$\lim_{X\to\pm\infty} C(X,Y,T) = 0, \quad \lim_{Y\to\infty} C(X,Y,T) = 0 \tag{18}$$

where $a = f(0)$. Now, the goal is to simplify the equation (15) by introducing a new unknown function, $v(X,Y,T)$ such that

$$C(X,Y,T) = \exp\left[\frac{u_0}{2D_0}(X+Y)\right] v(X,Y,T) \tag{19}$$

This reduces the ADE (15) with conditions (16) - (18) to

$$\frac{\partial v}{\partial T} = D_0\left(\frac{\partial^2 v}{\partial X^2} + \frac{\partial^2 v}{\partial Y^2}\right) - \frac{u_0^2}{2D_0} v \tag{20}$$

$$v(X,Y,0) = 0 \tag{21}$$

$$v(X,0,T) = \frac{C_0}{a}\delta(X)\delta(T) \tag{22}$$

$$\lim_{X\to\pm\infty} v(X,Y,T) = 0, \quad \lim_{Y\to\infty} v(X,Y,T) = 0 \tag{23}$$

Implementing CF time fractional derivative to ADE (20) yields

$${}^{CF}D_t^{\alpha} v(X,Y,T) = D_0 \frac{\partial^2 v(X,Y,T)}{\partial X^2} + D_0 \frac{\partial^2 v(X,Y,T)}{\partial Y^2} - \frac{u_0^2}{2D_0} v(X,Y,T) \tag{24}$$

To solve the fractional ADE (FADE) given in (24), the Laplace transform with respect to T, defined by $\bar{v}(X,Y,s) = \int_0^\infty v(X,Y,T)e^{-sT}\,ds$, is first applied. This is followed by the Sine-Fourier transform with respect to Y, given by $\tilde{\bar{v}}(X,\eta,s) = \sqrt{\frac{2}{\pi}}\int_{-\infty}^{\infty} \bar{v}(X,Y,s)\sin(\eta Y)\,dY$, and finally the exponential Fourier transform with respect to X, defined as $\tilde{\bar{v}}^*(\xi,\eta,s) = \int_{-\infty}^{\infty} \tilde{\bar{v}}(X,\eta,s)e^{-i\xi X}\,dX$. This transformations process yields the transformed equation

$$\tilde{\bar{v}}^*(\xi,\eta,s) = \sqrt{\frac{2}{\pi}}\frac{C_0}{a}\frac{D_0\eta}{\left[\frac{s\gamma}{s+\alpha\gamma} + D_0\eta^2 + D_0\xi^2 + \frac{{u_0}^2}{2D_0}\right]} \tag{25}$$

where $\gamma = \frac{1}{1-\alpha}$.

To facilitate the application of the inverse transformation, the term is expressed into auxiliary components in the form

$$\tilde{\bar{v}}^*(\xi,\eta,s) = \tilde{\bar{v}}_1^*(\xi,\eta,s) + \tilde{\bar{v}}_2^*(\xi,\eta,s) \tag{26}$$

where

$$\tilde{\bar{v}}_1^*(\xi,\eta,s) = \sqrt{\frac{2}{\pi}}\frac{D_0 C_0}{a}\left[\frac{\eta}{\left(D_0\eta^2 + D_0\xi^2 + \frac{{u_0}^2}{2D_0} + \gamma\right)}\right] \tag{27}$$

and

$$\tilde{\bar{v}}_2^*(\xi,\eta,s) = \sqrt{\frac{2}{\pi}}\eta\frac{C_0}{a}D_0\left[\frac{\alpha\gamma^2}{\left(D_0\eta^2+D_0\xi^2+\frac{u_0{}^2}{2D_0}+\gamma\right)^2}\frac{1}{\left[s+\frac{\alpha\gamma\left(D_0\eta^2+D_0\xi^2+\frac{u_0{}^2}{2D_0}\right)}{\left(D_0\eta^2+D_0\xi^2+\frac{u_0{}^2}{2D_0}+\gamma\right)}\right]}\right] \tag{28}$$

By applying the inverse integral transformations and utilizing symmetry properties of integrals, the results are obtained as

$$v_1(X,Y,T) = \frac{2}{\pi^2}D_0\frac{C_0}{a}\delta(T)\int_0^\infty\int_0^\infty \frac{\eta\sin(\eta Y)\cos(\xi X)}{\left(D_0\xi^2+D_0\eta^2+\frac{u_0^2}{2D_0}+\gamma\right)}d\eta\,d\xi \tag{29}$$

and

$$v_2(X,Y,T) = \frac{2}{\pi^2}\frac{C_0}{a}D_0\int_0^\infty\int_0^\infty \frac{\eta\alpha\gamma^2\sin(\eta Y)\cos(\xi X)}{\left(D_0\eta^2+D_0\xi^2+\frac{u_0^2}{2D_0}+\gamma\right)^2} \times\exp\left(-\frac{\alpha\gamma\left(D_0\eta^2+D_0\xi^2+\frac{u_0^2}{2D_0}\right)}{\left(D_0\eta^2+D_0\xi^2+\frac{u_0^2}{2D_0}+\gamma\right)}T\right)d\eta\,d\xi \tag{30}$$

The integral is in the ξ and η variables. Now, let

$$\xi = \rho\cos\theta\,, \quad \eta = \rho\sin\theta \tag{31}$$

where $\rho \in [0,\infty), \theta \in \left[0,\frac{\pi}{2}\right]$.

Therefore, $v_1(X,Y,T)$ converts to

$$v_1(X,Y,T) = \frac{2}{\pi^2}D_0\frac{C_0}{a}\delta(T)\int_0^\infty\int_0^{\frac{\pi}{2}} \frac{\rho^2}{\left(D_0\rho^2+\frac{u_0^2}{2D_0}+\gamma\right)}\sin\theta\sin[(\rho\sin\theta)Y]\cos[(\rho\cos\theta)X]\,d\rho\,d\theta \tag{32}$$

Then, let $z = \cos\theta$. For the integration part involving θ , it can be shown that

$$\int_0^{\frac{\pi}{2}}\sin\theta\sin[(\rho\sin\theta)Y]\cos[(\rho\cos\theta)X]\,d\theta = \int_0^1\sin\left(Y\rho\sqrt{1-z^2}\right)\cos(X\rho z)\,dz \tag{33}$$

According to [28],

$$\int_0^1\cos(mz)\sin\left(n\sqrt{1-z^2}\right)dz = \frac{\pi}{2}\left(\frac{n}{\sqrt{m^2+n^2}}\right)J_1\left(\sqrt{m^2+n^2}\right) \tag{34}$$

which relate to (33) such that $m = X\rho$ and $n = Y\rho$. Hence, (32) can be written as

$$v_1(X,Y,T) = \frac{YD_0C_0\delta(T)}{\alpha\pi\sqrt{X^2+Y^2}}\int_0^\infty \frac{\rho^2}{\left(D_0\rho^2 + \frac{u_0^2}{2D_0} + \gamma\right)} J_1\left(\rho\sqrt{X^2+Y^2}\right) d\rho \tag{35}$$

Using the same approach, $v_2(X,Y,T)$ converts to

$$\begin{aligned} &v_2(X,Y,T) \\ &= \frac{\alpha\gamma^2 YC_0D_0}{\alpha\pi\sqrt{X^2+Y^2}}\exp(-\alpha\gamma T) \\ &\times \int_0^\infty \frac{\rho^2}{\left(D_0\rho^2 + \frac{u_0}{2D_0} + \gamma\right)^2}\exp\left(\frac{\alpha\gamma^2 T}{D_0\rho^2 + \frac{u_0^2}{2D_0} + \gamma}\right) J_1\left(\rho\sqrt{X^2+Y^2}\right) d\rho \end{aligned} \tag{36}$$

Since $v_1(X,Y,T)$ contains delta function, $\delta(T)$ which suggests that it is only nonzero at $T = 0$

$$\delta(T) = \begin{cases} \infty, & T = 0 \\ 0, & T \neq 0 \end{cases} \tag{37}$$

Therefore, for $T > 0$, $v_1(X,Y,T) = 0$, resulting in

$$v(X,Y,T) = v_2(X,Y,T) \tag{38}$$

By using the identity of Bessel function $J_0(z) + J_2(z) = \frac{2}{z}J_1(z)$, (36) can be written as

$$\begin{aligned} &v(X,Y,T) \\ &= \frac{\alpha\gamma^2 YC_0D_0}{2\alpha\pi}\exp(-\alpha\gamma T) \\ &\times \int_0^\infty \frac{\rho^3}{\left(D_0\rho^2 + \frac{u_0^2}{2D_0} + \gamma\right)^2}\exp\left(\frac{\alpha\gamma^2 T}{D_0\rho^2 + \frac{u_0^2}{2D_0} + \gamma}\right)\Big[J_0\left(\rho\sqrt{X^2+Y^2}\right) \\ &+ J_2\left(\rho\sqrt{X^2+Y^2}\right)\Big] d\rho \end{aligned} \tag{39}$$

Finally, by substituting (39) into (19), the solution of FADE is obtained as

$$\begin{aligned} &C(X,Y,T) \\ &= \frac{\alpha\gamma^2 YC_0D_0}{2\alpha\pi}\exp\left[\frac{u_0}{2D_0}(X+Y) - \alpha\gamma T\right] \\ &\times \int_0^\infty \frac{\rho^3}{\left(D_0\rho^2 + \frac{u_0^2}{2D_0} + \gamma\right)^2}\exp\left(\frac{\alpha\gamma^2 T}{D_0\rho^2 + \frac{u_0^2}{2D_0} + \gamma}\right)\Big[J_0\left(\rho\sqrt{X^2+Y^2}\right) \\ &+ J_2\left(\rho\sqrt{X^2+Y^2}\right)\Big] d\rho, \quad Y > 0, T > 0 \end{aligned} \tag{40}$$

To examine the classical case, consider the limit of the CF derivative as $\alpha \to 1$ as given in Remark 1 (or, equivalent, $\gamma \to \infty$). From (40),

$$\lim_{\alpha\to 1} \frac{\alpha\gamma^2}{\left(D_0\rho^2+\frac{u_0^2}{2D_0}+\gamma\right)^2}\exp\left(-\alpha\gamma T+\frac{\alpha\gamma^2 T}{D_0\rho^2+\frac{u_0{}^2}{2D_0}+\gamma}\right)$$
$$=\lim_{\gamma\to\infty}\frac{\gamma^2}{\left(D_0\rho^2+\frac{u_0^2}{2D_0}+\gamma\right)^2}\exp\left(\frac{-\gamma T\left(D_0\rho^2+\frac{u_0^2}{2D_0}\right)}{D_0\rho^2+\frac{u_0{}^2}{2D_0}+\gamma}\right)$$
$$=\exp\left(-T\left(D_0\rho^2+\frac{u_0{}^2}{2D_0}\right)\right) \tag{41}$$

Therefore, the solution for classical ADE ($\alpha\to 1$)

$$C(X,Y,T)=\frac{YC_0D_0}{2a\pi}\exp\left[\frac{u_0}{2D_0}(X+Y)-\frac{u_0^2}{2D_0}T\right]\times\int_0^\infty \rho^2\exp(-D_0\rho^2T)\left[\frac{2J_1\left(\rho\sqrt{X+Y^2}\right)}{\sqrt{X+Y^2}}\right]d\rho \tag{42}$$

Using the formula $\int_0^\infty x^{v+1}e^{-ax^2}J_v(bx)dx=\frac{b^v}{(2a)^{v+1}}e^{-\frac{b^2}{4a}}, a>0, b>0, \mathrm{Re}(v)>-1$, the solution for classical ADE can be simplified as

$$C(X,Y,T)=\frac{YC_0}{4D_0T^2a\pi}\exp\left[\frac{u_0}{2D_0}(X+Y)-\frac{u_0^2}{2D_0}T-\frac{X^2+Y^2}{4D_0T}\right] \tag{43}$$

Numerical Simulations and Discussion

In order to analyse the influence of the fractional parameter α, on the advection-diffusion process, the concentration profiles given by the fractional solution (40) and the classical solution given by (43) are compared. Specially, in the following Figure 1 and 2, the fractional solutions are represented by $\alpha = 0.1, 0.2$ and 0.4, while the classical solution is represented by $\alpha = 1$. The parameter values listed in Table 1 are used, which are based on references relevant to river environments. Consider a scenario where a pollutant is instantaneously introduced into the river with concentration $C_0 = 1\ \mathrm{kg/m^3}$. The pollutant undergoes dispersion characterized by a diffusion coefficient D_0, while being advected downstream with a time-dependent river velocity given by $u = u_0\exp(-0.1\mathrm{t})$. The time dependent function $f(mt)$ is assumed to be in the form of $f(mt) = \exp(-mt)$ with $m = 0.1$.

Table 1. Diffusion and velocity parameter values based on references relevant to river environments

Parameter	Value	Reference
Diffusion, D_0	0.13 m^2/day	[29]
Velocity, u_0	0.05 m/day	[29]

Figure 1 illustrates the concentration profiles plotted along the spatial coordinate x for $y = 0.4$, six values of time t, and different values of the fractional parameter α. Overall, the results show a significant dependence of the concentration profiles on the fractional parameter α. For the fractional solutions, lower values of α result in lower concentrations, with decreasing peaks as time increases. Since the source is represented by a delta function located at $y = 0$, the concentration is seen to be localized at the centerline ($x = 0$), resulting in higher concentration levels at that location. It can also be seen that the classical solution produces the highest concentration at $t = 1$ day, but $\alpha = 0.4$ surpasses the classical solution by $t = 2$ day. At later times, the classical solution decreases again and ultimately drops below all the fractional solutions. When $\alpha = 1$, corresponding to the classical solution, the concentration keeps decreasing, followed by a completely flattened profile by $t = 15$ day.

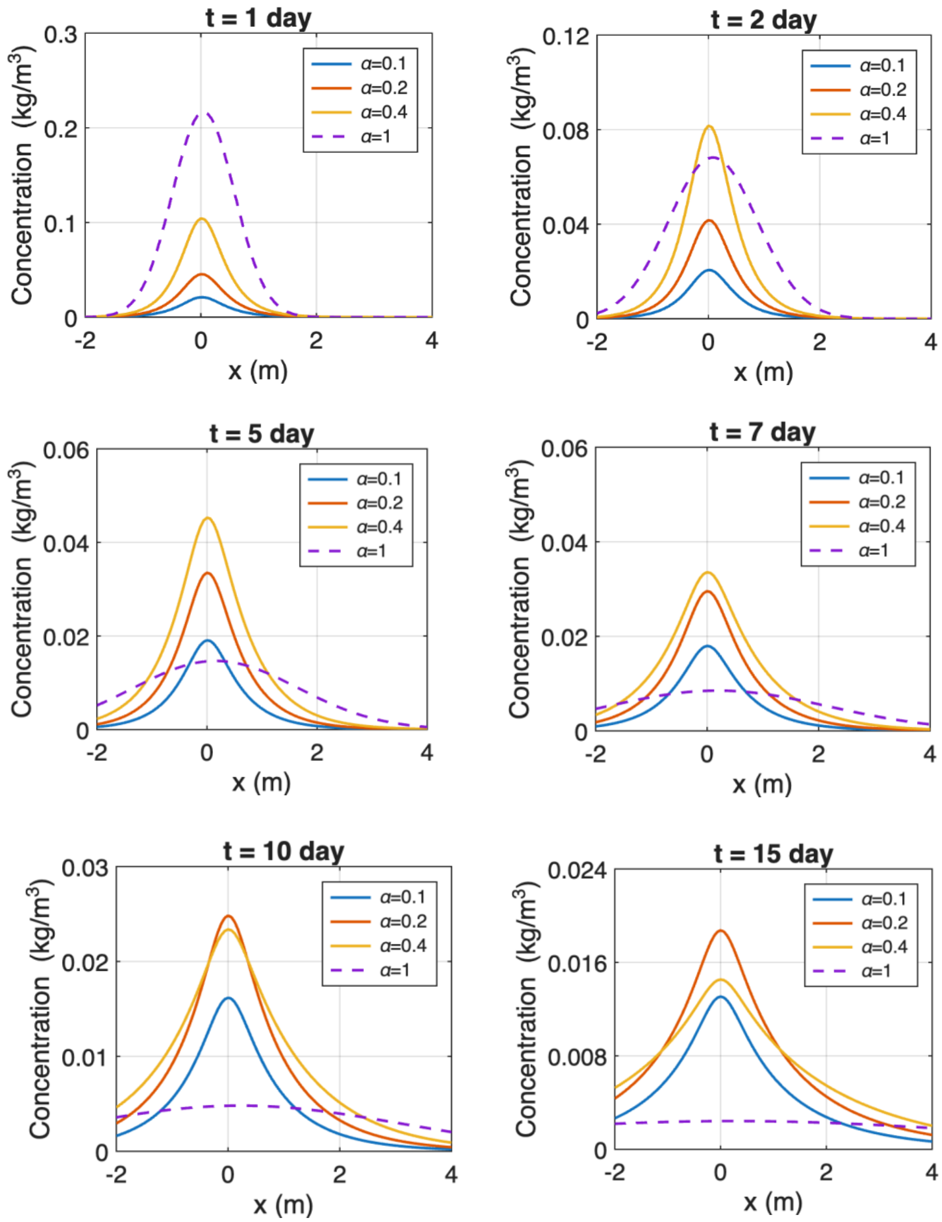

Figure 1 Concentration profiles along spatial coordinate x comparing the fractional solution ($\alpha < 1$, Eq. 40) with the classical solution ($\alpha = 1$, Eq. 43)

Figure 2 shows the concentration profiles along the y-direction at $x = 0$ for different fractional parameters α over various time. Similar to Figure 1, lower values of α result in lower concentration peaks, and the peaks decrease gradually as time progresses. At the early stages ($t = 1$ and 2 day), all profiles are sharply peaked near $y = 0$, with concentration rapidly decreasing downstream. By $t = 5$ day, the solution with $\alpha = 0.4$ surpasses the classical solution in peak concentration, indicating a temporary dominance of fractional transport at that time scale. By $t = 10$ day, the peak concentration of the classical solution drops below the peaks of the fractional profiles for $\alpha = 0.2$ and $\alpha = 0.4$. The classical solution shows continuously decreasingly peaks over time, transitioning towards a flattened profile, while the fractional solutions maintain a localized peak near the source ($x = y = 0$).

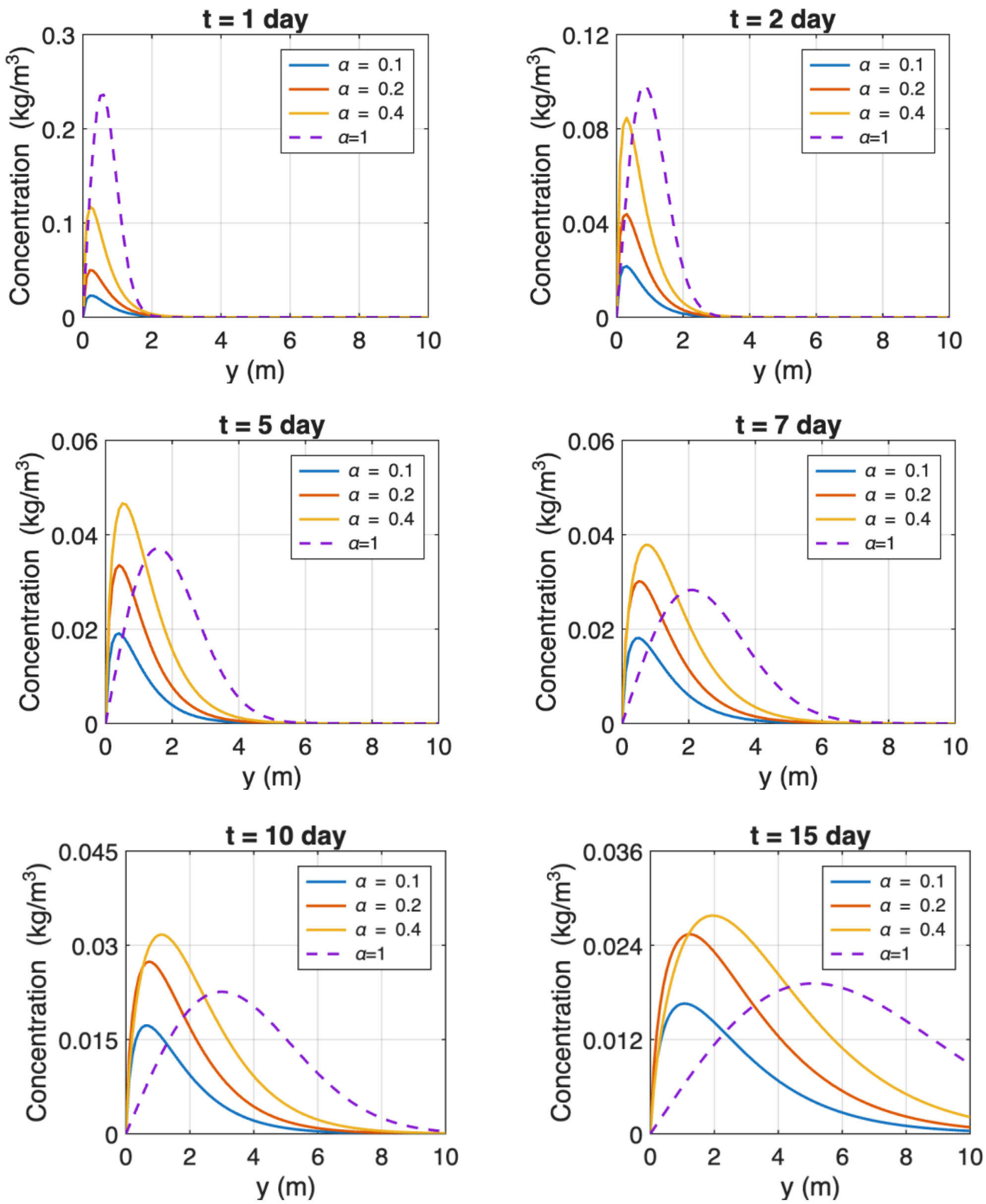

Figure 2 Concentration profiles along spatial coordinate y comparing the fractional solution ($\alpha < 1$, Eq. 40) with the classical solution ($\alpha = 1$, Eq. 43)

In this present study, the velocity is assumed to be time dependent. Figure 3 compares concentration profiles for both time-dependent velocity ($m = 0.1$) and constant velocity ($m = 0$) cases with fractional parameter $\alpha = 0.2$. At early time, the profiles for both $m = 0$ and $m = 0.1$ are nearly identical as the exponential term in the time-dependent velocity $u = u_0 \exp(-0.1t)$ remains close to 1. Hence, both velocity conditions result in almost the same concentration distribution. As time increases, the time-dependent velocity produces a significantly higher and broader peak concentration while constant velocity case exhibits lower peak concentration. This indicates that the varying velocity over time enhances the accumulation and dispersion of the pollutant more effectively than a steady, constant flow.

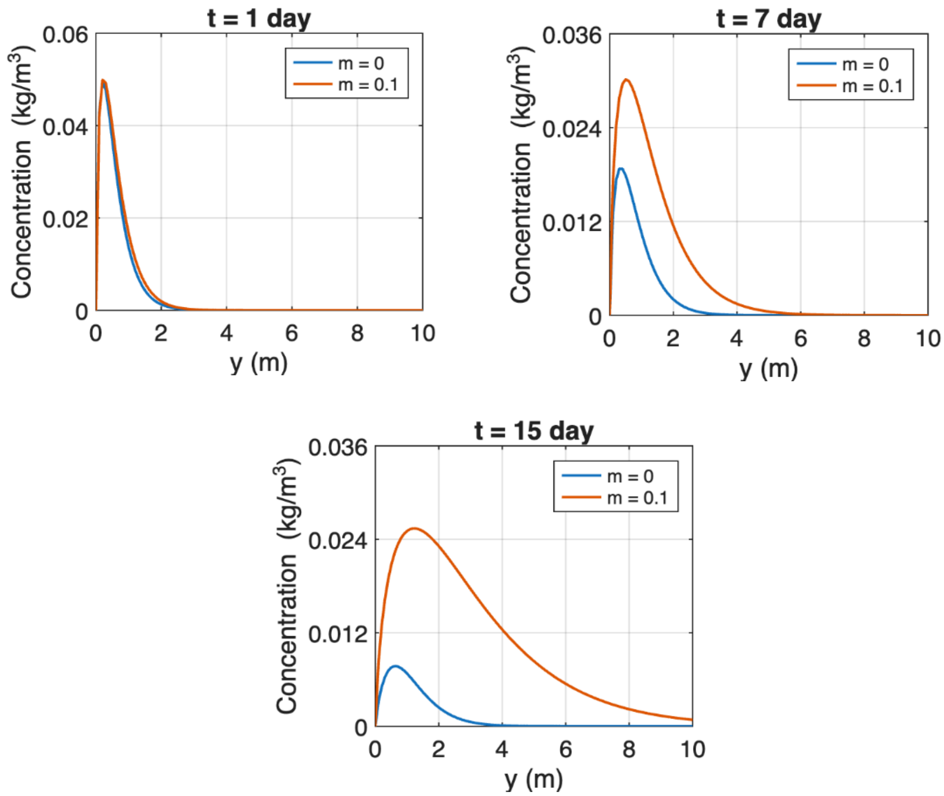

Figure 3 Comparison of concentration profiles for constant $(m = 0)$ and time-dependent $(m = 0.1)$ velocity for fractional parameter $\alpha = 0.2$.

Conclusions

This study demonstrates that the fractional parameter α and the choice of velocity (constant or time-dependent) significantly influence the concentration profiles in the two-dimensional advection-diffusion equation. As the fractional parameter α decreases, the overall concentration profiles decrease and produce lower peaks but maintain a localized concentration over time. Conversely, the classical solution leads to a flattened profile that moves further downstream as time increases. When comparing time-dependent and constant velocity cases, the time-dependent velocity consistently produces higher and broader concentration peaks due to the varying speed of transport. In contrast, the constant velocity case leads to a less dynamic spread of the concentration over time, with lower peak concentrations. These findings underscore the significance of incorporating both fractional modeling and time-dependent velocity to better represent real-world pollutant transport in dynamic and complex environments.

Conflicts of Interest

The authors declare that there is no conflict of interest regarding the publication of this paper.

Acknowledgment

This work is part of a research project with cost centre Q.J130000.2754.03K99 supported by Universiti Teknologi Malaysia.

References

[1] Manitcharoen, N., & Pimpunchat, B. (2020). Analytical and numerical solutions of pollution concentration with uniformly and exponentially increasing forms of sources. Journal of Applied Mathematics, 2020, 1-9.
[2] Paudel, K., Kafle, J., & Bhandari, P. S. (2022). Advection-Dispersion Equation for Concentrations of Pollutant and Dissolved Oxygen. Journal of Nepal Mathematical Society, 5(1), 30-40.

[3] Hadhouda, M. K., & Hassan, Z. S. (2022). Mathematical model for unsteady remediation of river pollution by aeration. Inf. Sci. Lett, 11-323.
[4] Gbenro, S. O., & Nchejane, J. N. (2022). Numerical Simulation of the Dispersion of Pollutant in a Canal. Asian Research Journal of Mathematics, 18(4), 25-40.
[5] Ruishi, L., & Isa, Z. M. (2023). Two-Dimensional Heavy Metal Migration in Soil with Adsorption and Instantaneous Injection. Malaysian Journal of Fundamental and Applied Sciences, 19(6), 980-988.
[6] Liang, R., & Isa, Z. M. (2024). Heavy metal transport with adsorption for instantaneous and exponential attenuation of concentration. Scientific Reports, 14(1), 537.
[7] Chaudhary, M., Thakur, C. K., & Singh, M. K. (2020a). Analysis of 1-D pollutant transport in semi-infinite groundwater reservoir. Environmental Earth Sciences, 79, 1-23.
[8] Jiang, J., Luo, H. H., Wang, S. F., Su, J., & Yu, Y. D. (2023). A two-dimensional analytical model for heavy metal contaminants transport in permeable reactive barrier. Water Science & Technology, 87(2), 393-406.
[9] Mustafa, S., Bahar, A., Abidin, A. R. Z., Aziz, Z. A., & Darwish, M. (2021). Three-dimensional model for solute transport induced by groundwater abstraction in river-aquifer systems. Alexandria Engineering Journal, 60(2), 2573-2582.
[10] Mustafa, S., Bahar, A., Aziz, Z. A., & Darwish, M. (2020). Solute transport modelling to manage groundwater pollution from surface water resources. Journal of contaminant hydrology, 233, 103662.
[11] Mustafa, S., Bahar, A., Aziz, Z. A., & Darwish, M. (2022). Analytical solutions of contaminant transport in homogeneous and isotropic aquifer in three-dimensional groundwater flow. Environmental Science and Pollution Research, 29(58), 87114-87131.
[12] Agarwal, R., Yadav, M. P., Agarwal, R. P., & Baleanu, D. (2019). Analytic solution of space time fractional advection dispersion equation with retardation for contaminant transport in porous media. Progress in Fractional Differentiation and Applications, 5(4), 1-13.
[13] Mainardi, F. (2023). Fractional Calculus and Waves in Linear Viscoelasticity: An Introduction to Mathematical Models. World Scientific.
[14] Mirza, I. A., & Vieru, D. (2017). Fundamental solutions to advection–diffusion equation with time-fractional Caputo–Fabrizio derivative. Computers & Mathematics with Applications, 73(1), 1-10.
[15] Ahmed, N., Shah, N. A., & Vieru, D. (2019). Two-dimensional advection–diffusion process with memory and concentrated source. Symmetry, 11(7), 879
[16] Mirza, I. A., Akram, M. S., Shah, N. A., Imtiaz, W., & Chung, J. D. (2021). Analytical solutions to the advection-diffusion equation with Atangana-Baleanu time-fractional derivative and a concentrated loading. Alexandria Engineering Journal, 60(1), 1199-1208.
[17] Jannelli, A. & Speciale, M. P (2021). Exact and numerical solutions of two-dimensional time-fractional diffusion–reaction equations through the Lie symmetries. Nonlinear Dynamics, 105, 2375–2385.
[18] Purohit, M., & Mushtaq, S. (2020). Applications of Laplace-Adomian decomposition method for solving time-fractional advection dispersion equation. J. Math. Comput. Sci., 10(5), 1960-1968.
[19] Sene, N. (2021). Fractional advection-dispersion equation described by the Caputo left generalized fractional derivative. Palestine J. Math, 10(2), 562-579.
[20] Ahmed, M., Zainab, Q. U. A., & Qamar, S. (2017). Analysis of One-Dimensional Advection–Diffusion Model with Variable Coefficients Describing Solute Transport in a Porous medium. Transport in Porous Media, 118, 327-344.
[21] Djordjevich, A., Savović, S., & Janićijević, A. (2017). Explicit finite-difference solution of two-dimensional solute transport with periodic flow in homogenous porous media. Journal of Hydrology and Hydromechanics, 65(4), 426-432.
[22] Das, P., Akhter, A., & Singh, M. K. (2018). Solute transport modelling with the variable temporally dependent boundary. Sādhanā, 43, 1-11.
[23] Yadav, R. R., & Kumar, L. K. (2019). Solute transport for pulse type input point source along temporally and spatially dependent flow. Pollution, 5(1), 53-70.
[24] Kumar, R., Chatterjee, A., Singh, M. K., & Tsai, F. T. (2022). Advances in analytical solutions for time-dependent solute transport model. Journal of Earth System Science, 131(2), 131.
[25] Jaiswal, D. K., Kumar, N., & Yadav, R. R. (2022). Analytical solution for transport of pollutant from time-dependent locations along groundwater. Journal of Hydrology, 610, 127826.
[26] Yang, S., Zhou, H., Zhang, S., & Wang, L. (2019). Analytical solutions of advective–dispersive transport in porous media involving conformable derivative. Applied Mathematics Letter, 92, 85-92.
[27] Yang, S., Chen, X., Ou, L., Cao, Y., & Zhou, H. (2020). Analytical solutions of conformable advection–diffusion equation for contaminant migration with isothermal adsorption. Applied Mathematics Letters, 105, 106330.
[28] Prudnikov, A.P., Brychkov, Yu. A., & Marichev, O.I. (1986). Integrals and Series Vol 1 Elementary Functions. Gordon and Breach Science Publishers
[29] Fazli, T. (2006). A Case Study of Sg. Skudai in the Comparison of River Water Quality Models in Total Maximum Daily Load Assessment. Master's thesis, Universiti Teknologi Malaysia.
[30] Qiao, C., Xu, Y., Zhao, W., Qian, J., Wu, Y., & Sun, H. (2020). Fractional derivative modeling on solute non-fickian transport in a single vertical fracture. *Frontiers in Physics*, *8*, 378.